

Accepted Manuscript

Title: Highly Transparent, Stretchable, and Rapid Self-Healing Polyvinyl Alcohol/Cellulose Nanofibril Hydrogel Sensors for Sensitive Pressure Sensing and Human Motion Detection

Authors: Xin Jing, Heng Li, Hao-Yang Mi, Yue-Jun Liu, Pei-Yong Feng, Yi-Min Tan, Lih-Sheng Turng



PII: S0925-4005(19)30793-2
DOI: <https://doi.org/10.1016/j.snb.2019.05.082>
Reference: SNB 26605

To appear in: *Sensors and Actuators B*

Received date: 22 January 2019
Revised date: 10 May 2019
Accepted date: 23 May 2019

Please cite this article as: Jing X, Li H, Mi H-Yang, Liu Y-Jun, Feng P-Yong, Tan Y-Min, Turng L-Sheng, Highly Transparent, Stretchable, and Rapid Self-Healing Polyvinyl Alcohol/Cellulose Nanofibril Hydrogel Sensors for Sensitive Pressure Sensing and Human Motion Detection, *Sensors and amp; Actuators: B. Chemical* (2019), <https://doi.org/10.1016/j.snb.2019.05.082>

This is a PDF file of an unedited manuscript that has been accepted for publication. As a service to our customers we are providing this early version of the manuscript. The manuscript will undergo copyediting, typesetting, and review of the resulting proof before it is published in its final form. Please note that during the production process errors may be discovered which could affect the content, and all legal disclaimers that apply to the journal pertain.

Highly Transparent, Stretchable, and Rapid Self-Healing Polyvinyl Alcohol/Cellulose Nanofibril Hydrogel Sensors for Sensitive Pressure Sensing and Human Motion Detection

Xin Jing^{1,2,3}, Heng Li⁴, Hao-Yang Mi^{1, 4*}, Yue-Jun Liu¹, Pei-Yong Feng¹, Yi-Min Tan¹, and Lih-Sheng Turng^{2,3*}

¹Key Laboratory of Advanced Packaging Materials and Technology of Hunan Province, Hunan University of Technology, Zhuzhou, Hunan, 412007, China

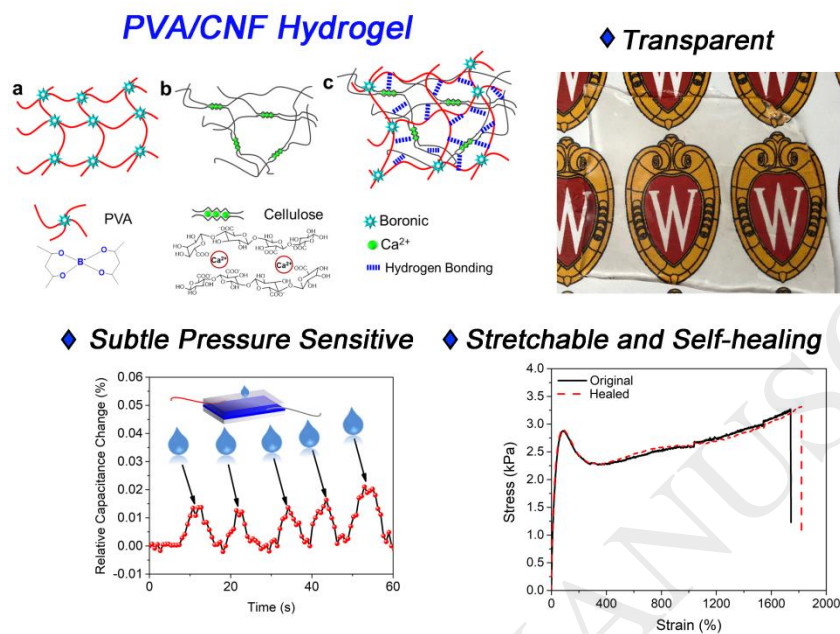
²Wisconsin Institute for Discovery, University of Wisconsin–Madison, Madison, Wisconsin 53715, United States

³Department of Mechanical Engineering, University of Wisconsin–Madison, Madison, Wisconsin 53706, United States

⁴Department of Building and Real Estate, Hong Kong Polytechnic University, Hong Kong, 518000, China

*Corresponding authors: Lih-Sheng Turng, email: turng@engr.wisc.edu, Tel: (608) 262-0586
Hao-Yang Mi, email: mhyscut@gmail.com, Tel: (0731) 2218 3805

Graphical abstract



Highlights

- The prepared hydrogel showed a great self-healing ability and spontaneously self-healed within 15 s
- The prepared hydrogel was highly transparent, with transmittance reaching as high as 90%.
- The developed hydrogel sensor was able to sense very subtle external pressure such as water drop
- The sensor worked stably on the detection of human motions such as finger, knee or elbow movements

Abstract

Wearable sensors have emerged as favored novel devices for human healthcare. Current sensors, however, suffer from low sensitivity, non-transparency, and lack of self-healing ability. In this study, we synthesized a polyvinyl alcohol/cellulose nanofibril (PVA/CNF) hydrogel with dual-crosslinked networks for highly transparent, stretchable, and self-healing pressure and strain sensors. The hydrogel contains dynamic borate bonds, metal–carboxylate coordination bonds, and hydrogen bonds, all of which contribute to the hydrogel's superior dimensional stability, mechanical strength and flexibility, and spontaneous self-healing ability as compared to traditional PVA hydrogels. The developed hydrogel has a moderate modulus of 11.2 kPa, and a high elongation rate of 1900%. It spontaneously self-heals within 15 s upon contact without any external stimuli, has a high transmittance of over 90%, and has excellent compatibility with human fibroblasts. The capacitive sensor developed based on the PVA/CNF hydrogel has high sensitivity to very subtle pressure changes, such as small water droplets. When used as a strain sensor, it was capable of detecting and monitoring various human motions such as finger, knee, elbow, and head movements, breathing, and gentle tapping. The developed hydrogel and sensors not only show great potential in electronic skin, personal healthcare, and wearable devices, but may also inspire the development of transparent, intelligent skin-like sensors.

Keywords: Stretchable hydrogel; Transparent; Self-healing; High sensitivity

1. Introduction

Nowadays, electronic skin and soft wearable sensors have attracted extensive attention due to their capacity to mimic human skin, which is self-healing, soft, robust, and able to sense subtle environmental differences[1-4] such as pressure[5-8], strain[9-14], temperature[15-17], humidity[18, 19], and forced deformation[20] via detectable electronic signals (current, resistance, or capacitance). These intelligent devices have been used in human motion detection, personalized health monitoring, and artificial intelligence[21-24]. However, developing materials with low elastic moduli and good stretchability still present profound challenges in the effort to fully mimic human skin due to skin's combination of mechanical and sensory properties[19, 25, 26]. Moreover, a soft artificial skin that is only flexible or stretchable is not sufficient for biomimetic purposes. It also needs to be (1) mechanically compliant and durable, (2) able to match curved surfaces, (3) sensitive to subtle changes, and (4) autonomously self-healing[27-29]. Suo et al. reported an artificial "ionic skin" based on chemically crosslinked polyacrylamide (PAM) hydrogels that integrated biocompatibility and stretchability[30, 31]. However, the ionic skin lacked the ability to self-heal and had poor interfacial contact.

Physically crosslinked hydrogels, which are deformable, stretchable, and autonomously self-healing, have highly attractive properties for the generation of artificial skin. Great efforts have been devoted to fabricating self-healing hydrogels based on noncovalent reactions and dynamic covalent interactions[32-35]. Bao et al. reported an elastic self-healing capacitive sensor based on a combination of dynamic metal-coordinated bonds and hydrogen bonds in a multiphase separated network[36]. Wang et al. developed a self-healable and stretchable electronic composite comprised of polyaniline, polyacrylic acid, and phytic acid by the combination of physical and chemical crosslinking[37]. Xing et al. reported a 3D printable and

self-healable composite hydrogel by employing dynamic ionic interactions between carboxyl acid and ferric ions, as well as chemical crosslinking, during the *in-situ* polymerization of polyacrylic acid[38]. However, in practical applications, most reported self-healing hydrogels are often plagued with problems such as long healing times[39, 40] or stimulus dependence[32, 33, 41, 42].

In addition to self-healing, transparency is also an important characteristic for soft artificial skin. Most developed hydrogel sensors are still opaque due to the loading of conductive fillers or polymers such as carbon nanotubes[43, 44], polyaniline[37], and poly(3,4-ethylene-dioxythiophene):polystyrene sulfonate (PEDOT:PSS)[45]. Regarding the characteristics of high stretchability, self-healing, and transparency, a polyvinyl alcohol (PVA) hydrogel might be a good candidate for compliant ionic skins compared to other materials. Zhang et al. reported an artificial epidermal skin sensor based on a composite of PVA/CNT/polydopamine[44]. Liu et al. also fabricated a PVA/PDA epidermal strain sensor with a high sensing performance at both ultralow and high strains (0.1~500%)[9]. The employment of a borate ion complex to the adjacent hydroxyl of PVA is a common way to fabricate PVA hydrogels with autonomously self-healing properties. However, due to the invertible nature of the borate bond, the PVA chains in the hydrogel remain mobile. This leads to weak mechanical properties and severely restricts their further application[46, 47].

Construction of another network is a desirable way to address this problem[48-50]. The metal–ligand coordination bond—a kind of noncovalent interaction—is desirable in biological systems for adjusting adhesion and stiffness[51-54]. Yang et al. demonstrated that metal–ligand interactions were able to associate and dissociate reversibly and rapidly, and could be used as physical crosslinkers for preparing high-strength hydrogels[55, 56].

Cellulose nanofibrils (CNFs), an abundant naturally occurring polysaccharide with a native crystalline structure, have attracted great interest as they are renewable, biocompatible, biodegradable, and abundant[57-59]. 2,2,6,6-Tetramethylpiperidine-1-oxyl (TEMPO)-mediated CNFs contain a large amount of carboxyl groups on their backbone chains. The presence of the carboxyl groups not only enriches raw material choices for finite components, but also facilitates the formation of noncovalent bonds in material systems[55].

In this study, we presented a highly sensitive, stretchable, mechanically compliant, and autonomously self-healing ionic skin using a dual-crosslinking hydrogel composed of polyvinyl alcohol (PVA) and 2,2,6,6-tetramethylpiperidine-1-oxyl radical (TEMPO)-oxidized cellulose nanofibrils (CNFs). Typically, CNFs introduce the first crosslinking network through ionic coordination bonds between Ca^{2+} and carboxylic groups from carboxylated CNFs. Then, a secondary crosslinking network is induced through dynamic borate bonding. The self-healing efficiency of the prepared ionic skin achieved 100% and was able to autonomously self-heal within 15 s without any external stimuli. The developed composite ionic skin integrates high stretchability, great sensitivity, good transparency, excellent biocompatibility, and quick self-healability, which are very attractive for the next generation of biosensors and artificially intelligent ionic skins.

2. Materials and Methods

2.1 Materials

Poly(vinyl alcohol) (M_w 89000~98000, >99% hydrolyzed) and calcium chloride were purchased from Sigma–Aldrich. Sodium tetraborate (assay 99.0%) was bought from Fisher Scientific. Cellulose nanofibril (CNF), a concentration of 1 wt% in water, was extracted from

eucalyptus Kraft pulp at Forest Products Laboratory (FPL, USA) using a TEMPO-oxidation method based on a previously reported method[60]. All aqueous solutions were prepared using deionized water (Milli-Q, Millipore Corp). All reagents were used as received.

2.2 Hydrogel Preparation

A quantity of calcium chloride was first mixed with a cellulose solution and then stored in a 4 °C refrigerator for 2 h to prepare the cellulose hydrogel. The optimized concentration of CaCl_2 was 2.5 mg/mL according to our preliminary tests. PVA powder was added into deionized water to prepare a 16% wt/v solution under stirring at 90 °C for 2 h. Meanwhile, an 8% wt. sodium borate solution was prepared by dissolving the sodium borate into the deionized water under stirring at 60 °C for 2 h. After the PVA solution was cooled down to room temperature, a defined volume of cellulose gel was added to the PVA solution to obtain a PVA/cellulose mixture under magnetic stirring. The weight ratio of the CNFs was controlled from 3.1% to 7.9% of the PVA by changing the volume of the CNF hydrogel. At last, the borax aqueous solution was mixed with the PVA/cellulose solution by gentle stirring using a spatula (to prevent introducing bubbles) until a gel was obtained, which was then named as PVA/cellulose D (where D refers to the dual-crosslinked networks, abbreviated as PVA/CNF D). The optimized weight ratio of PVA and borax was 6:1. For comparison, a pure PVA hydrogel was prepared using the same method.

2.3 Fabrication of a Pressure and Strain Sensor

The pressure sensor was composed of a dielectric layer and two conductive layers. In the sensor, the dielectric layer (polyethylene film with a thickness of 50 μm) was sandwiched between two hydrogel layers (with thicknesses of 1 mm) that acted as conductive layers connected to two metallic electrodes. Meanwhile, the top and bottom conductive hydrogel layers

were covered with two additional polyethylene layers to prevent water evaporation. Separately, Very High Bond tape (3M, VHB 4910, 2 mm thick) was used as a stretchable dielectric layer and sandwiched between the two hydrogel layers that were connected to two metallic electrodes to assemble the stretchable capacitive strain sensor for human motion detection. To prevent dehydration, the hydrogel layers were packed again with VHB tape. Thus, the two layers of hydrogels were basically sealed in three layers of VHB tape.

2.4 Characterization

2.4.1 FTIR, UV-Vis Spectroscopy

The FTIR spectra of PVA, cellulose before and after crosslinking, and freeze-dried hydrogels were recorded in transmittance mode using a Bruker Tensor 27 spectrometer (Thermo Scientific Instrument) in the range of 4000–600 cm^{-1} with a resolution of 4 cm^{-1} . The transparency of the hydrogel was characterized on a UV-Vis spectrophotometer (Cary 500 UV-Vis–NIR spectrophotometer) from 800 nm to 400 nm.

2.4.2 Morphological Characterization

The prepared hydrogels were freeze-dried to observe the morphologies and distribution of the cellulose fibrils. Before observation, the surface of the dried hydrogels was sputter-coated with a gold layer. Then, a fully digital scanning electron microscope, LEO GEMINI (Zeiss, Germany), at a voltage of 3 kV, was employed to perform the visualization.

2.4.3 Rheological Tests

The rheological properties of the hydrogels were evaluated by a TA AR 2000ex rheometer with parallel plates (diameter: 25 mm, gap: 500 μm). A customer-designed apparatus was used to confine the hydrogel between the parallel plates during the test. (1) The oscillatory frequency sweep was performed to determine the linear equilibrium modulus plateau of the

hydrogel with an angular frequency ranging from 0.1 to 100 rad/s at 22 °C. The preset strain was kept at 1%. (2) The oscillatory strain amplitude sweep test was performed to determine the linear viscoelastic region of the hydrogel over a sweep of 0.1% to 500% at a fixed frequency of 1 Hz at 22 °C. (3) The creep-recovery test was carried out to investigate the viscous and elastic responses at a constant stress of 30 Pa at 22 °C. The stress was applied for 30 s then suddenly removed, and the sample was allowed to recover for 60 s. (4) An alternate step strain sweep test was carried out to observe the healing ability of the hydrogels at a fixed angular frequency (10 rad/s). The amplitude strains were switched from a small strain ($\gamma = 1\%$) to a subsequent large strain (300%) over 100 s for every strain interval.

2.4.4 Mechanical Properties

The tensile test was performed at a speed of 100 mm/min using a universal tensile machine (Instron 5967, USA) with a 250 N load cell. The hydrogel was sized into 5 cm \times 1 cm \times 0.5 cm rectangular shapes prior to testing. Three samples were tested for each group.

2.4.5 Self-Healing Experiments

The hydrogels (5 cm \times 1 cm \times 0.5 cm) were cut into halves and then brought into contact to let them self-heal for 1 min without disturbance. After self-healing, tensile tests were carried out to evaluate their stretchable behavior.

2.4.6 Sensing Performance Characterization

An inductance, capacitance, and resistance (LCR) meter was used to perform capacitance measurements (879B, B&K Precision Corp., USA) at a 1 kHz frequency with a 1 V AC signal under various stimuli on the device.

To measure the pressure sensitivity, the assembled pressure sensor was compressed via a compression machine, and the compressive pressure was increased from 0 to 4 kPa in 1 min. The pressure sensitivity, S , was defined as the slope of the traces in the capacitance–pressure curve[5],

$$S = \delta(\Delta C / C_0) / \delta_p = (1/C_0) * \delta C / \delta p \quad (1)$$

where C and C_0 represent the capacitance before and after the applied pressure, respectively, and p refers to the applied pressure.

2.4.7 Biocompatibility Evaluation

HEF1, a human fibroblast-like cell type derived from human embryonic stem cells, was used as the cell model to investigate the biocompatibility of the hydrogel sensor. The detailed experimental procedures are shown in the Supporting Information.

3. Results and Discussion

Figure 1 (i) shows the schematic of the network formed via the reaction of the tetrafunctional borate ion and the –OH group of PVA. The crosslinking points in the hydrogel network are reversible and could be easily broken and reformed, which endowed the hydrogel with good self-healing and reforming abilities. However, due to the invertible bonding between borax and PVA (Figure 1 (a-i)), the hydrogel network remains mobile, thus leading to weak mechanical properties and limited stability of the hydrogel. This further restricts its wide application[46, 47]. Introducing a secondary network is a promising strategy to address this issue[48-50]. Therefore, cellulose nanofibrils (which are abundant in carboxyl groups) were employed to form the second network. Specifically, CNFs not only can be crosslinked via Ca^{2+} to form the second crosslinking networks (as shown in Figure 1 (a-ii)), they also induce the formation of hydrogen bonds with PVA chains, leading to the formation of interwoven

crosslinked networks, as shown in Figure 1 (iii). Figure S1 shows the hydrogel after resting for 1 h. It was found that the PVA hydrogel deformed significantly due to the dynamic network in the PVA hydrogel. In contrast, the PVA/CNF D hydrogel maintained its original shape well, which indicated the high stability of the PVA/CNF D hydrogel. To reveal the underlying mechanism, both hydrogels were freeze-dried and imaged using SEM. Figure 1 (b-d) shows their porous morphologies in which pores were left by the removal of water. Compared with the pores of the freeze-dried PVA hydrogel, the PVA/CNF D hydrogel exhibited smaller pores (Figure 1 (c)) and nanofibrils were observed both on the pore walls and inside the pores bridging the adjacent pore walls (Figure 1 (d)). This special hierarchical micro- and nano-scale structure of the PVA/CNF D hydrogel might be responsible for improving its mechanical stability.

Furthermore, FTIR was carried out to investigate interactions between CNFs and Ca^{2+} , the PVA and the tetra-functional borate ion, and CNFs and PVA. As shown in Figure 2 (a), The coordinate bonds between carboxyl groups of CNFs and Ca^{2+} can be substantiated by the shifting of the peak from 1600 to 1605 cm^{-1} and 1404 to 1430 cm^{-1} [61], respectively, which verifies the presence of the crosslinking network in the crosslinked CNFs. In Figure 2(b), a broad and strong peak centered around 3319 cm^{-1} was attributed to the stretching vibration of the $-\text{OH}$ groups, which were sensitive to hydrogen bonding. Compared to pure PVA, the $-\text{OH}$ stretching peak shifted to a higher wavenumber, and the intensity of the peak was enhanced in the PVA hydrogel, demonstrating the presence of hydrogen bonding between the borax and the PVA molecular chains[43, 62]. Moreover, after introducing CNFs into the hydrogels, the stretching peak of $-\text{OH}$ further shifted to 3348 cm^{-1} (as shown in Figure 2 (b)), thus indicating the appearance of

hydrogen bonding between CNFs and PVA, which would be beneficial for improving the mechanical properties, self-healing abilities, and dimensional stability of the hydrogel.

The crosslinking network in hydrogels significantly affects their mechanical properties. The tensile test results (Figure 2 (c)) showed that the pure PVA hydrogel had an elongation rate of 1605%, while the elongation rate of the PVA/CNF D hydrogel increased to 1919%. It should be noted that pure CNFs crosslinked rapidly when mixed with the CaCl_2 solution to form a brittle hydrogel with an elongation rate within 5% of strain (Figure S2). Thus, the dual-network hydrogel outperformed both pure hydrogels. Moreover, from the statistical results of the different hydrogels, it was found that both the tensile strength and tensile modulus of the PVA/CNF D hydrogel increased as the CNF ratio to PVA increased. However, when the ratio exceeded 6.3%, the hydrogel started to become brittle, as indicated by the significant decrease in elongation-at-break. Thus, the PVA/CNF D hydrogel containing 6.3% CNF was recognized as the optimum formula and was used for the rest of the experiments. Overall, the tensile modulus for the PVA/CNF D hydrogel was 12.6% higher than the modulus of the PVA hydrogel, the tensile strength was improved by 137.1%, and the hydrogel toughness was significantly enhanced by 220.4%. These results indicate a simultaneous improvement of strength and flexibility of the hydrogel by introducing dual-crosslinking networks, which is highly desirable for freestanding robust sensor applications. This improvement was attributed to the hydrogen bonding and the second crosslinking network formed between the cellulose and Ca^{2+} . Thus, the approach proposed here provides a new method for simultaneously reinforcing and toughening PVA hydrogels. In addition, the PVA/CNF D hydrogel maintained high transparency (over 90% to visible light) after the addition of CNF and the introduction of the dual-crosslinking network,

although the transparency was lower than that of the pure PVA hydrogel (over 95% to visible light).

The difference in molecular structures and interactions is reflected by their viscoelastic properties. Thus, the dynamic mechanical measurements were carried out on the CNF solution, CNF hydrogel, pure PVA hydrogel, and PVA/CNF D hydrogel to reveal the contribution of the dual-crosslinking network on the viscoelastic properties of hydrogels. The storage modulus G' and loss modulus G'' of the CNF solution and the CNF hydrogel were relatively independent of the frequency throughout the whole range, demonstrating the formation of a gel-like network [63]. The significantly higher storage modulus of the CNF hydrogel shown in Figure S3 indicates a denser and stronger network structure after introducing Ca^{2+} ions as crosslinkers in the CNF solution. For the pure PVA and PVA/CNF D hydrogels (Figure 3 (a)), both G' and G'' of the PVA/CNF D hydrogel were higher than the PVA hydrogel, which implies a stronger crosslinking network. A crossover frequency, which indicates the transition from liquid-like behavior to solid-like behavior, was observed in the PVA hydrogel. [64, 65] However, the G' of the PVA/CNF D hydrogel was higher than the G'' in the tested frequency range. This indicates that the dual crosslinking network effectively enhanced the stiffness and stability of the hydrogel. In the strain sweep measurement, the G' and G'' of the PVA/CNF D hydrogel were also higher than that of the PVA hydrogel, as shown in Figure 3 (b). As the strain ratio increased, G' and G'' decreased rapidly and G' intersected with G'' due to the collapse of the network in the hydrogels. The intersection strain for the PVA/CNF D hydrogel was 57.8%, while it was only 18.3% for the PVA hydrogel. This indicated that the dimensional stability of the hydrogel improved with the introduction of the CNF networks.[66] A steady state flow test was performed to investigate the

yield stress of the hydrogels. As shown in Figure S4, both the viscosity and shear stress of the PVA/CNF D hydrogel were superior to that of the PVA hydrogel. However, the yield was not detected since the hydrogel slipped and tended to move out from the parallel plates at a high strain rate.

In addition, creep and recovery tests were carried out to investigate the viscous and elastic responses when the hydrogels were subjected to a constant stress (creep) followed by a sudden release of the stress (recovery). From Figure 3 (c), it was found that the strain change of the PVA hydrogel was significantly greater than the PVA/CNF D hydrogel at a stress of 30 Pa, which further verified the stiffer network of the PVA/CNF D hydrogel. The degree of the recovered strain (γ_{rec}) for the PVA hydrogel was 38.2%, while the γ_{rec} was 52.6% for the PVA/CNF D hydrogel. This indicates that the dual crosslinking network improved the recoverability from the deformation of the hydrogel. Figure 3 (d) shows the alternate strain sweep test results of the PVA/CNF D hydrogel. When the hydrogel was subjected to 300% strain, the G' sharply decreased and the G'' became higher, indicating the collapse of the hydrogel network. When the strain was reduced to 1%, both G' and G'' returned to their original values. These breakage and recovery behaviors were repeated a couple of times and both G' and G'' maintained a stable trend, thus verifying the good self-healing efficiency of the PVA/CNF D hydrogel.

To demonstrate the rapid self-healing properties of the PVA/CNF D hydrogel, one piece of hydrogel was cut and healed three times in different directions. For the healing process, two pieces of hydrogels were simply brought into contact with one another at room temperature without any external stimuli. As shown in Figure S5, the hydrogel fully and rapidly recovered to its original state after each cut, indicating an isotropic structure and high self-healing ability. To further investigate the self-healing behavior, the cutting area was observed using an optical

microscope. As shown in Figure 3 (e), the self-healing process happened rapidly and the two parts were fully healed in 15 s. This rapid spontaneous self-healing behavior implies that the crosslinking sites quickly reestablished and this process induced the movement of molecular chains in the healing area. In order to study the effectiveness of the self-healing process, the tensile properties of the PVA/CNF D hydrogel were tested before and after self-healing. It can be seen from Figure 3 (f) that the tensile curves of the original and healed hydrogels almost overlapped, indicating that the self-healing process was highly efficient and the reestablished crosslinking bonds fully resembled the original bonds. Although some PVA and CNF molecular chains may be permanently destroyed by cutting, maintaining the mechanical properties implies that the dual-crosslinking networks played a major role in governing the mechanical performance of the hydrogel.

After fully characterizing the chemical and physical properties of this newly developed PVA/CNF D hydrogel, we investigated its potential applications in pressure and strain sensing, as well as wearable human motion detection sensors. It is known that capacitance devices have high pressure and strain sensitivity and no inherent temperature sensitivity[2]. To investigate the potential sensing applications of the developed PVA/CNF D hydrogels, they were assembled into a capacitive sensor comprised of two layers of hydrogels as electrodes, with one layer of dielectric material sandwiched between them, as illustrated in Figure 4 (a). As shown in Figure S6, the conductivity of the hydrogel increased as the CNF ratio in the hydrogel increased due to the increase of Na^+ , Ca^{2+} , and Cl^- ions at a higher CNF ratio. Once the assembled sensor was connected to a capacitive meter, the ions in the hydrogel were redistributed due to the

electrostatic potential provided by the external battery. The relationship between deformation and capacitance in a parallel-plate configuration is shown in Equation (2),

$$C = \varepsilon S / 4\pi k d \quad (2)$$

where C is the capacitance, ε is the dielectric constant of the dielectric layer, S is the working area of the conducting layer, k is the electrostatic constant, and d is the thickness. Thus, any change in the dimension of the sensor would lead to a change in the capacitance of the sensor.

As shown in Figure 4 (b and c), the fabricated sensor was essentially a thin, transparent, flexible, and stretchable capacitor that used hydrogels as electrodes. Physical flexibility and optical transparency of sensors are highly desirable for wearable devices. We first investigated the pressure sensing performance of the sensor. A thin polyethylene terephthalate (PET) film was used as the dielectric layer of the sensor, and the sensor was sealed with a thin polyethylene (PE) film to prevent hydrogel dehydration (Figure 4(c)). The change in the thickness of the hydrogel, or the dimension of the sensor caused by external pressure exerted on the sensor, will lead to obvious changes in the capacitance (Figure 4 (d)). The dependence of the capacitance change of the sensor on the external force was tested via a compression machine. As shown in Figure 4 (e), it was found that the capacitance change was linearly related to the compressive pressure, and that the slope of the trace (known as the sensitivity, S , of the sensor) was 0.75 kPa^{-1} . This was almost 4.4 times more sensitive than the pure PVA hydrogel (shown in Figure S7), and it was four times higher than traditional chemically crosslinked PAM hydrogels[7]. This superior sensitivity was due to the CaCl_2 content and the Na^+ from the CNF. Moreover, the CNF/PVA D hydrogel-based sensors had superior sensitivity compared to other capacitive sensors developed in recent publications (see Table S2 for the comparison). Next, we tested the ability of the sensor to detect subtle pressure changes. We dropped small water droplets (weight of 30 mg, falling

from 15 cm) onto the surface of the sensor. The signal of the water drop was well reflected by the change in capacitance, as shown in Figure 4 (f), although the relative capacitive change for one water droplet was only about 0.02%. Moreover, if the electrode layer was replaced by the PVA hydrogel, it failed to detect the water droplets. This indicates that the PVA/CNF D hydrogel is highly promising for practical sensing applications.

Next, the tensile strain sensitivity of the hydrogel was investigated using a Very High Bond (VHB) tape as a stretchable dielectric layer. The sensor was packed by VHB tape to prevent hydrogel dehydration. Upon stretching, the dimensions of the sensor change distinctly, leading to a dramatic change in capacitance (Figure 4 (g)). The dependence of the capacitance on the stretching stress was studied by applying different stresses on the sensor. It was found that the capacitance change showed a nearly linear increase at a constant stress (0.5 kPa, 1 kPa, and 2 kPa), as shown in Figure S8, which implies that the sensor has high stability in detecting tensional force and deformation. To further demonstrate the sensing performance of the sensor in detecting cyclical motions, it was stretched to 500% strain and released to 0% strain for five cycles. As shown in Figure 4 (h), the sensor loading–unloading curves almost overlapped in the five cycles, thus indicating a nearly 100% recovery rate of the developed sensor and a small energy dissipation in each cycle. It also demonstrated the high mechanical property stability of the sensor when subjected to repetitive large motions. The signal detected from the loading–unloading motion (Figure 4 (i)) showed a highly regular and repetitive pattern that exactly reflected the stretching and releasing motion of the tensile test machine. Therefore, the developed sensors are highly sensitive and possess stable performance in repetitive measurements. To investigate the stability of the sensors over the long term, especially the effect of dehydration, the sensitivity of the sensor was measured over four weeks of storage in air. It

was found that the reduction of pressure sensitivity was only 13% after four weeks, which was attributed to the proper sealing of the hydrogels (Figure S9a). In addition, the effect of layer thickness was also investigated by varying the thickness of the hydrogel. It was found that increasing the hydrogel thickness from 1 mm to 2 mm had a negligible effect on sensor sensitivity (Figure S9b). This was because the charges were mainly aggregated near the surface of the hydrogel in the capacitive sensor.

. (e) The relative capacitance change of the PVA/CNF D hydrogel over a pressure range of 0~4 kPa. (f) Real-time capacitance changes upon water falling onto the pressure sensor. The arrows were used to indicate the instant the water made contact with the hydrogel. (g) Illustration of the capacitance change of sensor upon stretching. (h). The cyclic tensile test results of assembled sensor. (i) The relative capacitance change of sensor upon cyclic tensile tests.

For the application of wearable devices, it would be favorable to use biocompatible materials in case of direct contact with human skin. To verify the biocompatibility of the hydrogels we developed, HEF1 fibroblast cells were used as the cell model and seeded on the surface of the hydrogels for up to 10 days. Cell viability and proliferation were investigated at day 3 and day 10 time points. It was found that fibroblast cells were able to grow on both PVA hydrogel and PVA/CNF D hydrogels, and the cells showed a typical spread morphology with visibly elongated filopodia on the developed substrates, especially for cells living on the PVA/CNF D hydrogel (as indicated in Figure 5 (b) and (d)). This indicates that the cells showed a flourishing living state on the substrates. The number of cells increased significantly from day 3 to day 10, and the cell population on the PVA/CNF D hydrogel was significantly higher than cells on the PVA hydrogel (Figure 5 (e)). Moreover, the cell viability results showed that over 90%

of the cells were alive at day 3 on both hydrogels, and the viability further increased to over 95% by day 10, which implies that both hydrogels were highly biocompatible and are safe for human cells. Thus, they not only can be used in direct contact with human skin, but also have the potential to be used in biomedical devices and applications involving direct tissue contact.

Given their high biocompatibility, PVA/CNF D hydrogel sensors were used to detect human motions and complicated muscle movements. The sensor had the capability to detect and monitor various human activities. As shown in Figure 6 (a), the sensor was attached to the index finger, and the capacitance increased when the finger bent, while the capacitance remained unchanged until the finger was straight again. This process was repeated multiple times and the capacitance signal showed no obvious changes, thus indicating a reliable long-term sensing performance. When used as a pressure sensor, the hydrogel sensor was able to detect a very gentle finger touch, as shown in Figure 6 (b), where an instant sharp increase of capacitance was recorded. This implies that the hydrogels can be assembled into tactile panels to fabricate smart wearable keyboards. Moreover, when the sensor was attached to one's throat, it was able to detect neck movement. As shown in Figure 6 (c), the capacitance increased by 170% when the wearer's head tilts up and down. When the sensor was attached to the wrist, it was able to detect the change of blood flow as the tester made a fist (shown in Figure 6 (d)).

In addition, the sensor was also attached to a puppet's elbow and knee to investigate the sensitivity of the sensor to smaller amplitude motions. As shown in Figure S10, it was found that the sensor showed a strong and stable capacitance signal change in response to the different motions of the puppet. Furthermore, we also found that the sensor's sensitivity could be retained

after the self-healing process. After the two fractured parts were put in contact and spontaneously self-repaired, the healed sensor could be used to detect the finger motion (Figure S11), and the same single pattern was obtained as compared to the original sensor (Figure 6 (a)). Importantly, all of the sensing signals showed highly stable patterns, and baseline shifts were observed even in long-term repetitive measurements. This indicates that no permanent deformation, dehydration, or ion redistribution happened during the measurement. It also implies a high robustness of the sensors fabricated in this study. Therefore, the PVA/CNF D hydrogel-based sensor has great potential as a highly sensitive pressure and strain sensor for personal healthcare, wearable devices, and artificial intelligence applications.

4. Conclusions

In summary, we developed a PVA/CNF dual-crosslinked hydrogel that was highly stretchable, transparent, and biocompatible, and was used as a capacitive ionic skin sensor for detection of strain and pressure in this study. The hydrogel contained a dynamic PVA–borate network with metal coordinate bonds between carboxyl groups of CNFs and Ca^{2+} ions. Together with the hydrogen bonding between the PVA and CNFs, this novel PVA/CNF D hydrogel showed a spontaneous self-healing ability without the need for external stimuli. The introduction of a CNF secondary network not only improved the dimensional stability, mechanical strength, and viscoelasticity, but also endowed the hydrogel-based capacitive sensor with high sensitivity and remarkable stability. When used as a pressure sensor, the PVA/CNF D hydrogel-based sensor was able to sense very subtle pressures, such as a gentle finger touch, small water droplets, and human breathing. When used as a strain sensor, it was able to monitor human motion. Moreover, the sensing performance was maintained after self-healing. Therefore, the hydrogel

developed has great potential in applications such as artificial intelligence, personal healthcare, and wearable devices.

Acknowledgements

The authors would like to acknowledge the financial support of the Kuo K. and Cindy F. Wang Professorship, the Vice Chancellor for Research and Graduate Education (VCRGE) Office, the College of Engineering, the International Postdoctoral Exchange Fellowship Program, the National Natural Science Foundation of China (21604026; 51603075), and the Fundamental Research Funds for the Central Universities (2017BQ069). Great appreciation is given to the Wisconsin Institute for Discovery at University of Wisconsin–Madison for the research platforms.

5. References

- [1] M.L. Hammock, A. Chortos, B.C.K. Tee, J.B.H. Tok, Z.A. Bao, 25th Anniversary Article: The Evolution of Electronic Skin (E-Skin): a Brief History, Design Considerations, and Recent Progress, *Adv Mater*, 25(2013) 5997-6037.
- [2] A. Chortos, Z.N. Bao, Skin-inspired electronic devices, *Mater Today*, 17(2014) 321-31.
- [3] X.D. Wang, L. Dong, H.L. Zhang, R.M. Yu, C.F. Pan, Z.L. Wang, Recent progress in electronic skin, *Adv Sci*, 2(2015) 1500169.
- [4] H. Liu, W.J. Huang, X.R. Yang, K. Dai, G.Q. Zheng, C.T. Liu, et al., Organic vapor sensing behaviors of conductive thermoplastic polyurethane-graphene nanocomposites, *J Mater Chem C*, 4(2016) 4459-69.

- [5] S.C.B. Mannsfeld, B.C.K. Tee, R.M. Stoltenberg, C.V.H.H. Chen, S. Barman, B.V.O. Muir, et al., Highly sensitive flexible pressure sensors with microstructured rubber dielectric layers, *Nat Mater*, 9(2010) 859-64.
- [6] B.Y. Lee, J. Kim, H. Kim, C. Kim, S.D. Lee, Low-cost flexible pressure sensor based on dielectric elastomer film with micro-pores, *Sensor Actuat a-Phys*, 240(2016) 103-9.
- [7] Z.Y. Lei, Q.K. Wang, S.T. Sun, W.C. Zhu, P.Y. Wu, A Bioinspired Mineral Hydrogel as a Self-Healable, Mechanically Adaptable Ionic Skin for Highly Sensitive Pressure Sensing, *Adv Mater*, 29(2017) 1700321.
- [8] H. Liu, M.Y. Dong, W.J. Huang, J.C. Gao, K. Dai, J. Guo, et al., Lightweight conductive graphene/thermoplastic polyurethane foams with ultrahigh compressibility for piezoresistive sensing, *J Mater Chem C*, 5(2017) 73-83.
- [9] S.Q. Liu, R.M. Zheng, S. Chen, Y.H. Wu, H.Z. Liu, P.P. Wang, et al., A compliant, self-adhesive and self-healing wearable hydrogel as epidermal strain sensor, *J Mater Chem C*, 6(2018) 4183-90.
- [10] J.Y. Sun, Y.A. Zhao, Z.G. Yang, J.J. Shen, E. Cabrera, M.J. Lertola, et al., Highly stretchable and ultrathin nanopaper composites for epidermal strain sensors, *Nanotechnology*, 29(2018) 355304.
- [11] C. Hu, Z.Y. Li, Y.L. Wang, J.C. Gao, K. Dai, G.Q. Zheng, et al., Comparative assessment of the strain-sensing behaviors of polylactic acid nanocomposites: reduced graphene oxide or carbon nanotubes, *J Mater Chem C*, 5(2017) 2318-28.
- [12] Y. Cao, T.G. Morrissey, E. Acome, S.I. Allec, B.M. Wong, C. Keplinger, et al., A Transparent, Self-Healing, Highly Stretchable Ionic Conductor, *Adv Mater*, 29(2017).

- [13] C.Y. Shao, M. Wang, L. Meng, H.L. Chang, B. Wang, F. Xu, et al., Mussel-Inspired Cellulose Nanocomposite Tough Hydrogels with Synergistic Self-Healing, Adhesive, and Strain-Sensitive Properties, *Chem Mater*, 30(2018) 3110-21.
- [14] Y.H. Li, B. Zhou, G.Q. Zheng, X.H. Liu, T.X. Li, C. Yan, et al., Continuously prepared highly conductive and stretchable SWNT/MWNT synergistically composited electrospun thermoplastic polyurethane yarns for wearable sensing, *J Mater Chem C*, 6(2018) 2258-69.
- [15] J. Jeon, H.B.R. Lee, Z. Bao, Flexible Wireless Temperature Sensors Based on Ni Microparticle-Filled Binary Polymer Composites, *Adv Mater*, 25(2013) 850-5.
- [16] R.C. Webb, A.P. Bonifas, A. Behnaz, Y.H. Zhang, K.J. Yu, H.Y. Cheng, et al., Ultrathin conformal devices for precise and continuous thermal characterization of human skin (vol 12, pg 938, 2013), *Nat Mater*, 12(2013) 1078-.
- [17] C.H. Yang, B.H. Chen, J.X. Zhou, Y.M. Chen, Z.G. Suo, Electroluminescence of Giant Stretchability, *Adv Mater*, 28(2016) 4480-+.
- [18] Y. Pang, J.M. Jian, T. Tu, Z. Yang, J. Ling, Y.X. Li, et al., Wearable humidity sensor based on porous graphene network for respiration monitoring, *Biosens Bioelectron*, 116(2018) 123-9.
- [19] A. Chortos, J. Liu, Z.A. Bao, Pursuing prosthetic electronic skin, *Nat Mater*, 15(2016) 937-50.
- [20] Y.C. Lai, J.N. Deng, S.M. Niu, W.B. Peng, C.S. Wu, R.Y. Liu, et al., Electric Eel-Skin-Inspired Mechanically Durable and Super-Stretchable Nanogenerator for Deformable Power Source and Fully Autonomous Conformable Electronic-Skin Applications, *Adv Mater*, 28(2016) 10024-32.

- [21] Y.P. Zang, F.J. Zhang, C.A. Di, D.B. Zhu, Advances of flexible pressure sensors toward artificial intelligence and health care applications, *Mater Horiz*, 2(2015) 140-56.
- [22] B.X. Xu, A. Akhtar, Y.H. Liu, H. Chen, W.H. Yeo, S.I.I. Park, et al., An Epidermal Stimulation and Sensing Platform for Sensorimotor Prosthetic Control, Management of Lower Back Exertion, and Electrical Muscle Activation, *Adv Mater*, 28(2016) 4462-71.
- [23] J. Kim, M. Lee, H.J. Shim, R. Ghaffari, H.R. Cho, D. Son, et al., Stretchable silicon nanoribbon electronics for skin prosthesis, *Nat Commun*, 5(2014) 5747.
- [24] D. Son, J. Lee, S. Qiao, R. Ghaffari, J. Kim, J.E. Lee, et al., Multifunctional wearable devices for diagnosis and therapy of movement disorders, *Nat Nanotechnol*, 9(2014) 397-404.
- [25] T.P. Huynh, P. Sonar, H. Haick, Advanced Materials for Use in Soft Self-Healing Devices, *Adv Mater*, 29(2017).
- [26] D.D. Chen, D.R. Wang, Y. Yang, Q.Y. Huang, S.J. Zhu, Z.J. Zheng, Self-Healing Materials for Next-Generation Energy Harvesting and Storage Devices, *Adv Energy Mater*, 7(2017) 1700890.
- [27] S.J. Benight, C. Wang, J.B.H. Tok, Z.A. Bao, Stretchable and self-healing polymers and devices for electronic skin, *Prog Polym Sci*, 38(2013) 1961-77.
- [28] D.H. Kim, J.Z. Song, W.M. Choi, H.S. Kim, R.H. Kim, Z.J. Liu, et al., Materials and noncoplanar mesh designs for integrated circuits with linear elastic responses to extreme mechanical deformations, *P Natl Acad Sci USA*, 105(2008) 18675-80.
- [29] T. Someya, Z.N. Bao, G.G. Malliaras, The rise of plastic bioelectronics, *Nature*, 540(2016) 379-85.
- [30] C. Keplinger, J.Y. Sun, C.C. Foo, P. Rothemund, G.M. Whitesides, Z.G. Suo, Stretchable, Transparent, Ionic Conductors, *Science*, 341(2013) 984-7.

- [31] J.Y. Sun, C. Keplinger, G.M. Whitesides, Z.G. Suo, Ionic Skin, *Adv Mater*, 26(2014) 7608-14.
- [32] Y.Z. Guo, X. Zhou, Q.Q. Tang, H. Bao, G.C. Wang, P. Saha, A self-healable and easily recyclable supramolecular hydrogel electrolyte for flexible supercapacitors, *J Mater Chem A*, 4(2016) 8769-76.
- [33] Q. Chen, L. Zhu, H. Chen, H.L. Yan, L.N. Huang, J. Yang, et al., A Novel Design Strategy for Fully Physically Linked Double Network Hydrogels with Tough, Fatigue Resistant, and Self-Healing Properties, *Adv Funct Mater*, 25(2015) 1598-607.
- [34] Z. Wei, J.H. Yang, Z.Q. Liu, F. Xu, J.X. Zhou, M. Zrinyi, et al., Novel Biocompatible Polysaccharide-Based Self-Healing Hydrogel, *Adv Funct Mater*, 25(2015) 1352-9.
- [35] M. Krogsgaard, M.A. Behrens, J.S. Pedersen, H. Birkedal, Self-Healing Mussel-Inspired Multi-pH-Responsive Hydrogels, *Biomacromolecules*, 14(2013) 297-301.
- [36] Q.H. Zhang, S.M. Niu, L. Wang, J. Lopez, S.C. Chen, Y.F. Cai, et al., An Elastic Autonomous Self-Healing Capacitive Sensor Based on a Dynamic Dual Crosslinked Chemical System, *Adv Mater*, (2018) e1801435
- [37] T. Wang, Y. Zhang, Q.C. Liu, W. Cheng, X.R. Wang, L.J. Pan, et al., A Self-Healable, Highly Stretchable, and Solution Processable Conductive Polymer Composite for Ultrasensitive Strain and Pressure Sensing, *Adv Funct Mater*, 28(2018) 1705551.
- [38] M.A. Darabi, A. Khosrozadeh, R. Mbeleck, Y.Q. Liu, Q. Chang, J.Z. Jiang, et al., Skin-Inspired Multifunctional Autonomic-Intrinsic Conductive Self-Healing Hydrogels with Pressure Sensitivity, Stretchability, and 3D Printability *Adv Mater*, 30(2018) 1700533.
- [39] M. Nakahata, Y. Takashima, H. Yamaguchi, A. Harada, Redox-responsive self-healing materials formed from host-guest polymers, *Nat Commun*, 2(2011) 511.

- [40] B. Rybtchinski, Adaptive Supramolecular Nanomaterials Based on Strong Noncovalent Interactions, *Acs Nano*, 5(2011) 6791-818.
- [41] H.J. Zhang, H.S. Xia, Y. Zhao, Poly(vinyl alcohol) Hydrogel Can Autonomously Self-Heal, *Acs Macro Lett*, 1(2012) 1233-6.
- [42] Z.Q. Li, Z.H. Hou, H.X. Fan, H.R. Li, Organic-Inorganic Hierarchical Self-Assembly into Robust Luminescent Supramolecular Hydrogel, *Adv Funct Mater*, 27(2017).
- [43] G.F. Cai, J.X. Wang, K. Qian, J.W. Chen, S.H. Li, P.S. Lee, Extremely Stretchable Strain Sensors Based on Conductive Self-Healing Dynamic Cross-Links Hydrogels for Human-Motion Detection, *Adv Sci*, 4(2017) 1600190.
- [44] M.H. Liao, P.B. Wan, J.R. Wen, M. Gong, X.X. Wu, Y.G. Wang, et al., Wearable, Healable, and Adhesive Epidermal Sensors Assembled from Mussel-Inspired Conductive Hybrid Hydrogel Framework, *Adv Funct Mater*, 27(2017) 1703852.
- [45] Q.F. Rong, W.W. Lei, L. Chen, Y.A. Yin, J.J. Zhou, M.J. Liu, Anti-freezing, Conductive Self-healing Organohydrogels with Stable Strain-Sensitivity at Subzero Temperatures, *Angew Chem Int Edit*, 56(2017) 14159-63.
- [46] Q. Chen, L. Zhu, C. Zhao, Q.M. Wang, J. Zheng, A Robust, One-Pot Synthesis of Highly Mechanical and Recoverable Double Network Hydrogels Using Thermoreversible Sol-Gel Polysaccharide, *Adv Mater*, 25(2013) 4171-6.
- [47] J.P. Gong, Y. Katsuyama, T. Kurokawa, Y. Osada, Double-network hydrogels with extremely high mechanical strength, *Adv Mater*, 15(2003) 1155-8.
- [48] W.P. Chen, D.Z. Hao, W.J. Hao, X.L. Guo, L. Jiang, Hydrogel with Ultrafast Self-Healing Property Both in Air and Underwater, *Acs Appl Mater Inter*, 10(2018) 1258-65.

- [49] H. Chen, Q. Chen, R.D. Hu, H. Wang, B.M.Z. Newby, Y. Chang, et al., Mechanically strong hybrid double network hydrogels with antifouling properties, *J Mater Chem B*, 3(2015) 5426-35.
- [50] P. Zhu, M. Hu, Y.H. Deng, C.Y. Wang, One-Pot Fabrication of a Novel Agar-Polyacrylamide/Graphene Oxide Nanocomposite Double Network Hydrogel with High Mechanical Properties, *Adv Eng Mater*, 18(2016) 1799-807.
- [51] B.P. Lee, S. Konst, Novel Hydrogel Actuator Inspired by Reversible Mussel Adhesive Protein Chemistry, *Adv Mater*, 26(2014) 3415-9.
- [52] Y. Hu, Z.S. Du, X.L. Deng, T. Wang, Z.H. Yang, W.Y. Zhou, et al., Dual Physically Cross-Linked Hydrogels with High Stretchability, Toughness, and Good Self-Recoverability, *Macromolecules*, 49(2016) 5660-8.
- [53] Q. Chen, X.Q. Yan, L. Zhu, H. Chen, B. Jiang, D.D. Wei, et al., Improvement of Mechanical Strength and Fatigue Resistance of Double Network Hydrogels by Ionic Coordination Interactions, *Chem Mater*, 28(2016) 5710-20.
- [54] S. Xia, S.X. Song, G.H. Gao, Robust and flexible strain sensors based on dual physically cross-linked double network hydrogels for monitoring human-motion, *Chem Eng J*, 354(2018) 817-24.
- [55] C.Y. Shao, H.L. Chang, M. Wang, F. Xu, J. Yang, High-Strength, Tough, and Self-Healing Nanocomposite Physical Hydrogels Based on the Synergistic Effects of Dynamic Hydrogen Bond and Dual Coordination Bonds, *Acs Appl Mater Inter*, 9(2017) 28305-18.
- [56] J. Yang, F. Xu, C.R. Han, Metal Ion Mediated Cellulose Nanofibrils Transient Network in Covalently Cross-linked Hydrogels: Mechanistic Insight into Morphology and Dynamics, *Biomacromolecules*, 18(2017) 1019-28.

- [57] R.J. Moon, A. Martini, J. Nairn, J. Simonsen, J. Youngblood, Cellulose nanomaterials review: structure, properties and nanocomposites, *Chem Soc Rev*, 40(2011) 3941-94.
- [58] Y. Habibi, L.A. Lucia, O.J. Rojas, Cellulose Nanocrystals: Chemistry, Self-Assembly, and Applications, *Chem Rev*, 110(2010) 3479-500.
- [59] D. Klemm, F. Kramer, S. Moritz, T. Lindstrom, M. Ankerfors, D. Gray, et al., Nanocelluloses: A New Family of Nature-Based Materials, *Angew Chem Int Edit*, 50(2011) 5438-66.
- [60] H.Y. Mi, X. Jing, A.L. Politowicz, E. Chen, H.X. Huang, L.S. Turng, Highly compressible ultra-light anisotropic cellulose/graphene aerogel fabricated by bidirectional freeze drying for selective oil absorption, *Carbon*, 132(2018) 199-209.
- [61] N. Lin, C. Bruzzese, A. Dufresne, TEMPO-Oxidized Nanocellulose Participating as Crosslinking Aid for Alginate-Based Sponges, *Acs Appl Mater Inter*, 4(2012) 4948-59.
- [62] X.D. Qi, X.L. Yao, S. Deng, T.N. Zhou, Q. Fu, Water-induced shape memory effect of graphene oxide reinforced polyvinyl alcohol nanocomposites, *J Mater Chem A*, 2(2014) 2240-9.
- [63] J.Y. Huang, Y.K. Lai, F. Pan, L. Yang, H. Wang, K.Q. Zhang, et al., Multifunctional Superamphiphobic TiO₂ Nanostructure Surfaces with Facile Wettability and Adhesion Engineering, *Small*, 10(2014) 4865-73.
- [64] N. Sahiner, M. Singh, D. De Kee, V.T. John, G.L. McPherson, Rheological characterization of a charged cationic hydrogel network across the gelation boundary, *Polymer*, 47(2006) 1124-31.

- [65] L.H. Weng, X.M. Chen, W.L. Chen, Rheological characterization of in situ crosslinkable hydrogels formulated from oxidized dextran and N-carboxyethyl chitosan, *Biomacromolecules*, 8(2007) 1109-15.
- [66] T. Inoue, K. Osaki, Rheological Properties Of Poly(Vinyl Alcohol)/Sodium Borate Aqueous-Solutions, *Rheol Acta*, 32(1993) 550-5.

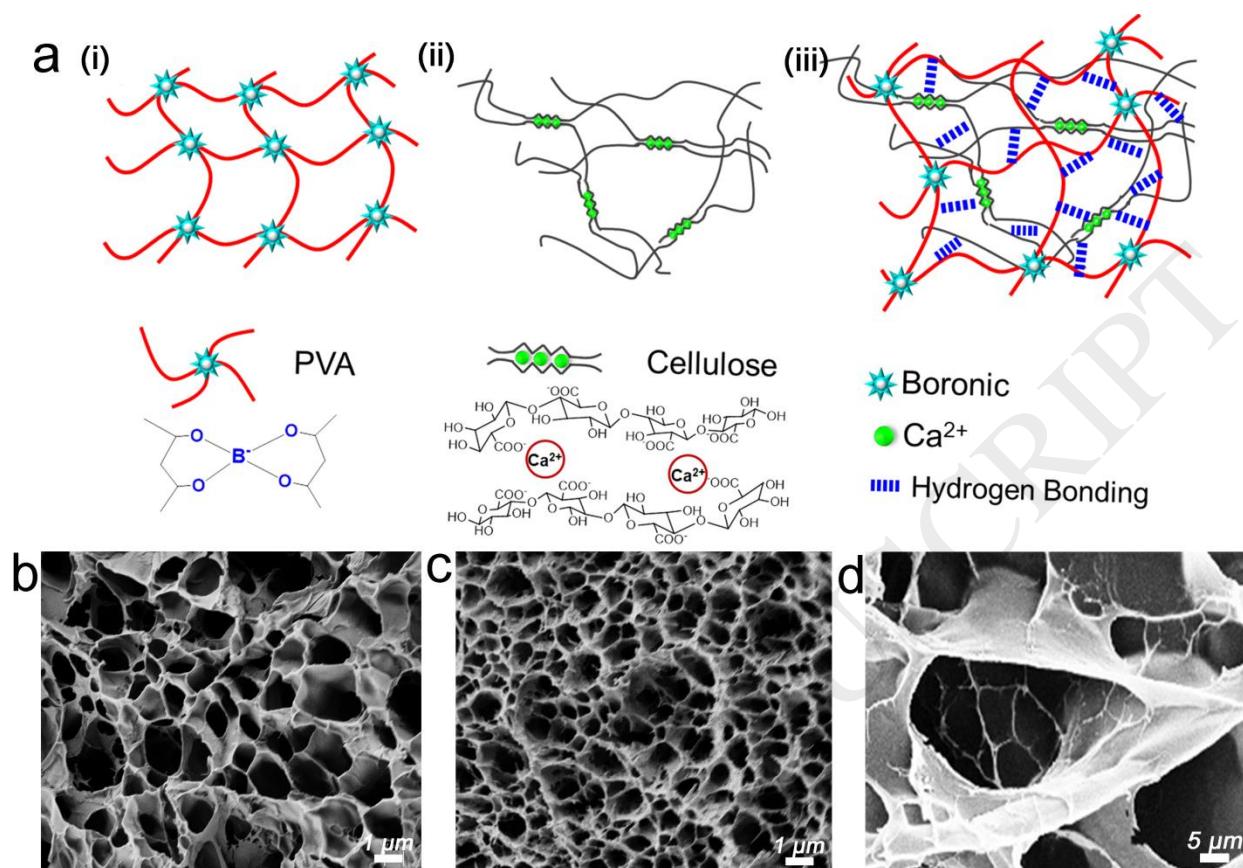


Figure 1. (a) Structure of the hydrogel network: (i) PVA hydrogel, (ii) CNF network, and (iii) PVA/CNF D hydrogel network schematics. (b) Morphologies of the freeze-dried PVA hydrogel; the scale bar is 1 μm . (c) and (d) Morphologies of the freeze-dried PVA/CNF D hydrogel; the scale bars are 1 μm and 5 μm , respectively.

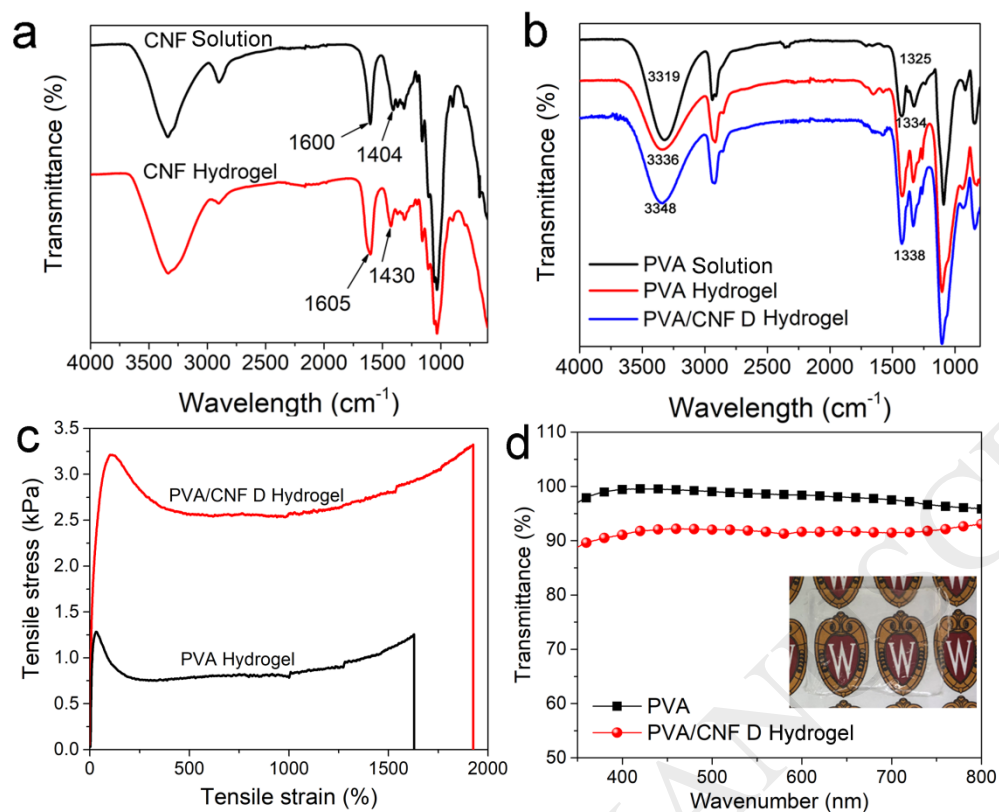


Figure 2. The FTIR results of (a) CNF and CNF hydrogel, and (b) PVA, PVA hydrogel, and PVA/CNF D hydrogel. (c) The representative tensile stress–strain curves of PVA hydrogel and PVA/CNF D hydrogel. (d) The transparent behavior of PVA hydrogel and PVA/CNF D hydrogel. The inset shows a digital photo of the PVA/CNF D hydrogel.

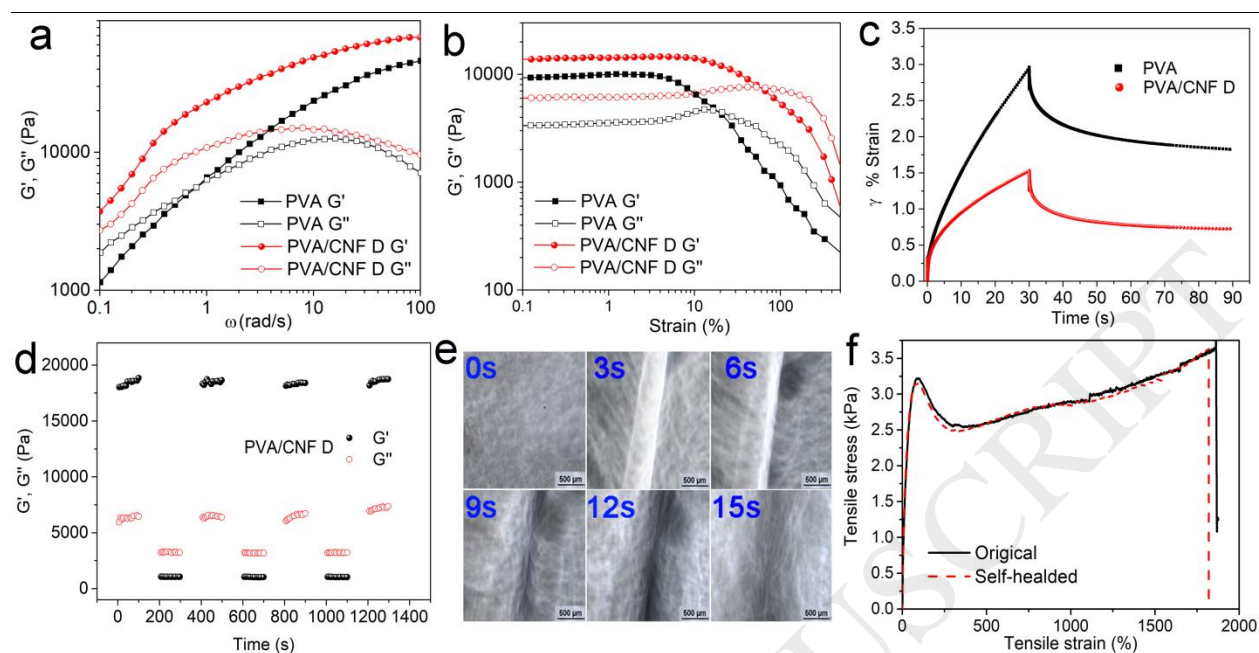


Figure 3. (a) G' and G'' of the PVA hydrogel and PVA/CNF D hydrogel in the oscillatory frequency sweep test. (b) G' and G'' of the PVA hydrogel and PVA/CNF D hydrogel in the oscillatory strain sweep test. (c) Creep-recovery results of the PVA hydrogel and PVA/CNF D hydrogel. (d) G' and G'' of the PVA/CNF D hydrogel in the alternate strain sweep test. (e) Optical images of the PVA/CNF D hydrogel during the self-healing process. The scale bar is 500 μ m. (f) Representative tensile stress-strain curves of the PVA/CNF D hydrogel before and after self-healing

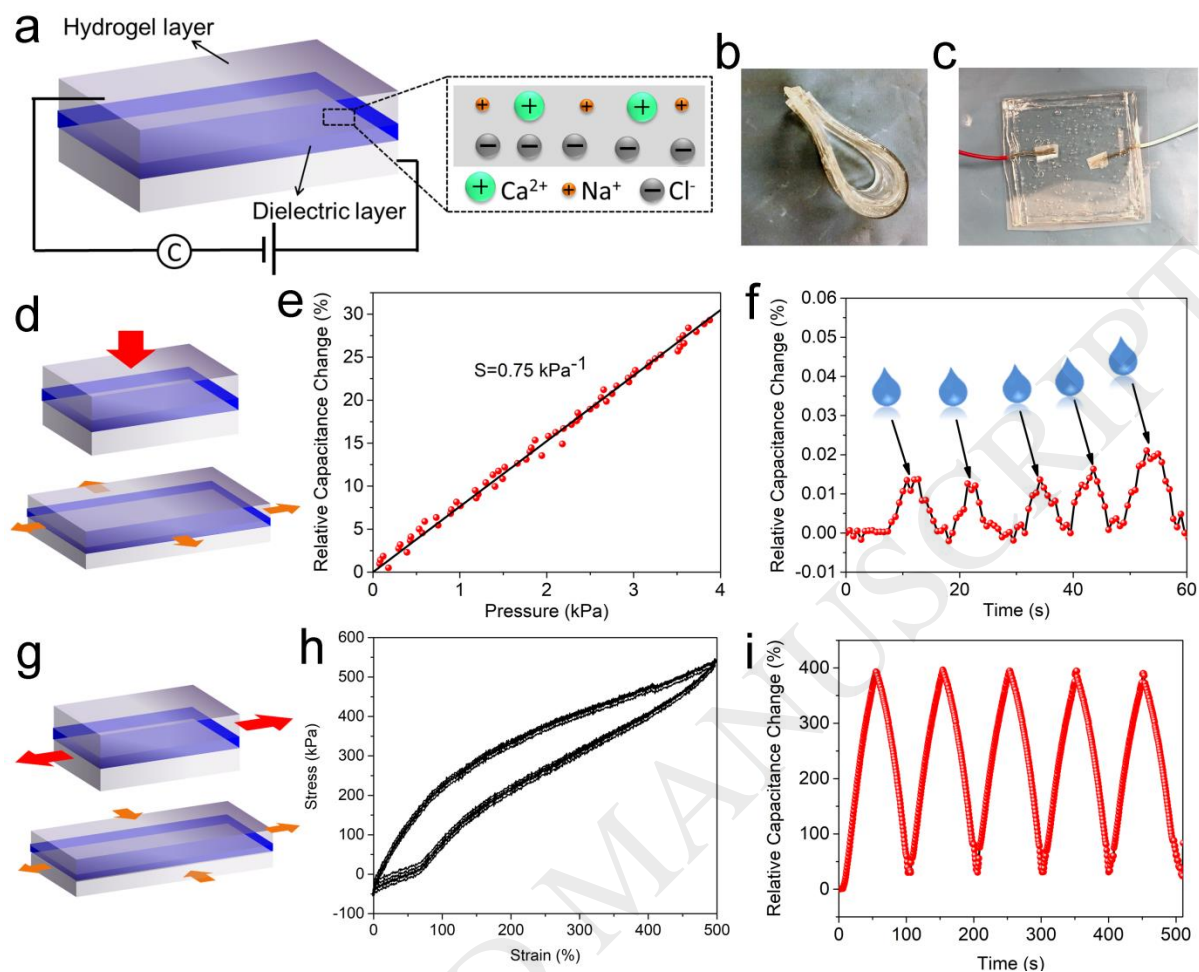


Figure 4. (a) The schematic design of the transparent ionic skin sensor. (b) A photo of the PVA/CNF D hydrogel-based ionic skin upon bending. (c) A photo of a water droplet falling onto the pressure sensor. (d) Illustration of the capacitance change of sensor upon pressure.

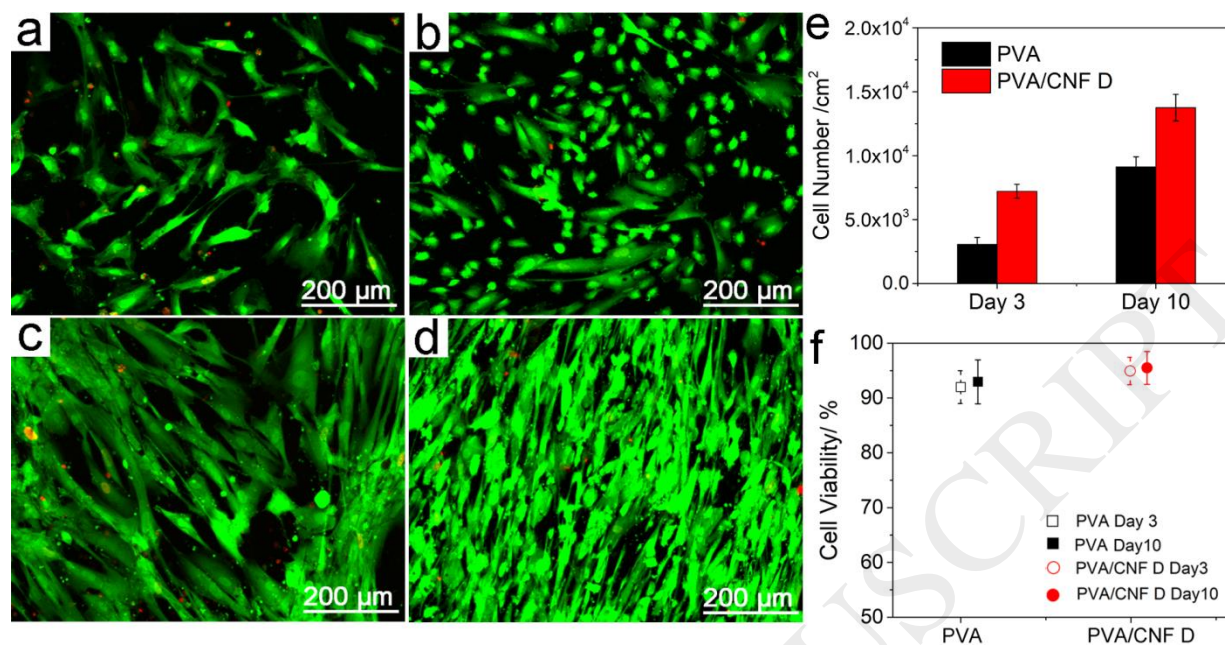


Figure 5. Live/dead images of HEF1 cells cultured on (a) PVA day 3, (b) PVA/CNF D day 3, (c) PVA day 10, and (d) PVA/CNF D day 10 hydrogels. The scale bar was 200 μm . The green fluorescence indicates live cells and the red color signifies dead cells. (e) The cell proliferation state on the hydrogels was evaluated by MTS assay. (f) Cell viability based on live/dead assay images.

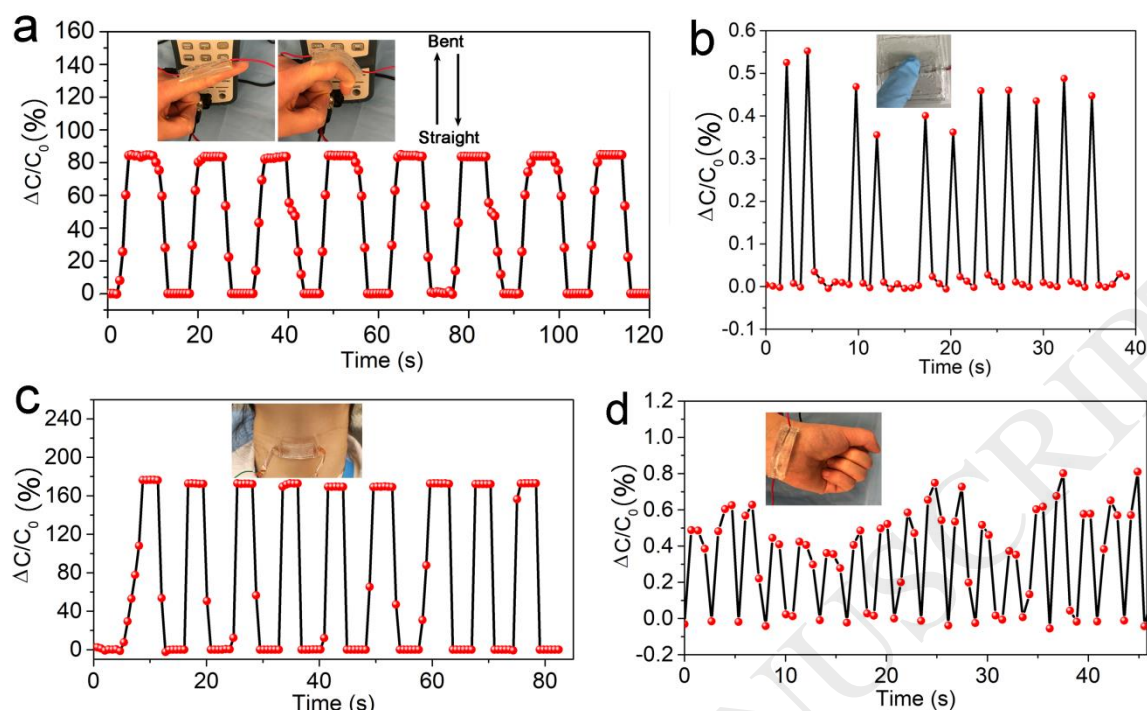


Figure 6. (a) Photos of hydrogel sensors attached to forefingers and used to detect the motions of the forefinger. (b) The response of the hydrogel sensors upon a gentle touch by a forefinger. (c) The real-time capacitance change of the hydrogel sensor attached to the throat to detect head movement. (d) Real-time capacitance signals when the hydrogel sensor was attached to a pulse point.